Available online at www.sciencedirect.com
ScienceDirect
Bioorganic & Medicinal Chemistry Letters 18 (2008) 3641–3645
Bioorganic & Medicinal Chemistry Letters

Lead identification to generate isoquinolinedione inhibitors of insulin-like growth factor receptor (IGF-1R) for potential use in cancer treatment

Scott C. Mayer,[a,*] Annette L. Banker,[a] Frank Boschelli,[d] Li Di,[a] Mark Johnson,[b] Cynthia Hess Kenny,[c] Girija Krishnamurthy,[c] Kristina Kutterer,[c] Franklin Moy,[b] Susan Petusky,[a] Malini Ravi,[c] Diane Tkach,[d] Hwei-Ru Tsou[c] and Weixin Xu[b]

[a]*Wyeth Research, Chemical & Screening Sciences, 865 Ridge Road, Monmouth Junction, Princeton, NJ 08852, USA*
[b]*Wyeth Research, Chemical & Screening Sciences, Cambridge, MA, USA*
[c]*Wyeth Research, Chemical & Screening Sciences, Pearl River, NY, USA*
[d]*Wyeth Research, Oncology, Pearl River, NY, USA*

Received 7 March 2008; revised 18 April 2008; accepted 21 April 2008
Available online 25 April 2008

Abstract—Insulin-like growth factor receptor (IGF-1R) is a growth factor receptor tyrosine kinase that acts as a critical mediator of cell proliferation and survival. This receptor is over-expressed or activated in tumor cells and is emerging as a novel target in cancer therapy. Efforts in our ''Hit to Lead'' group have generated a novel series of submicromolar IGF-1R inhibitors based on a isoquinolinedione template originating from a Lance enzyme HTS screen. Chemical triage and parallel synthesis incorporating focused library arrays were instrumental in moving these investigations through the Wyeth exploratory medicinal chemistry process. The strategies, synthesis, and SAR behind this interesting kinase scaffold will be described.

Receptor tyrosine kinases are proven targets for therapeutic intervention in human cancer.[1] As a member of this class of signaling molecules, the insulin-like growth factor receptor tyrosine kinase (IGF-1R) is a pivotal element of a signaling pathway involved in cell growth, proliferation, and survival.[2] It is highly related to the insulin receptor (IR) yet plays a different role in organism development, being responsible for normal growth and development as opposed to glucose homeostasis.[3] Several studies indicate that the IGF-1 receptor is overexpressed in human cancers, and plays a essential role in tumorigenesis.[4] Several experimental approaches to reducing IGF-1R levels have been reported, and the results suggest that tumor cell proliferation, survival and sensitivity to cytotoxic agents are dependent on the presence of IGF-1R. These effects are believed to result from downregulating PI3K and Ras pathways.[5] Inhibitors of IGF-1R kinase activity may therefore be suitable agents for inhibition of human tumor growth.

Efforts from our ''Hit to Lead'' group were aimed at developing selective small molecule inhibitors of IGF-1R for the treatment of cancer. The most significant challenge for the team would be obtaining selectivity over IR due to homology of these two receptors (IGF-1R has 84% sequence identity to IR in the kinase domain).[6]

A high-throughput screen (HTS) using a Lance enzyme assay[7] was performed generating 5359 confirmed hits. Through chemical triage and follow-on assays, full hit characterization was completed in a few months generating a novel kinase template; the isoquinolinedione series met all criteria as a viable lead and provided an unique scaffold for SAR development [compound **1** (Fig. 1)].[8] Along with chemical triage and data-mining, input from structural biology helped to fully characterize this lead series. Fluorescence data

Keywords: IGFR inhibitor; Isoquinolinedione; 'Hit to Lead' investigations.
* Corresponding author. Tel.: +1 732 274 4457; fax: +1 732 274 4505; e-mail: mayers@wyeth.com

0960-894X/$ - see front matter © 2008 Elsevier Ltd. All rights reserved.
doi:10.1016/j.bmcl.2008.04.044

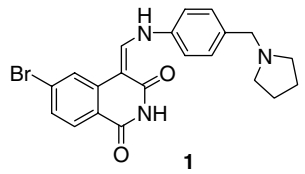

Figure 1. Representative compound from isoquinolinedione cluster.

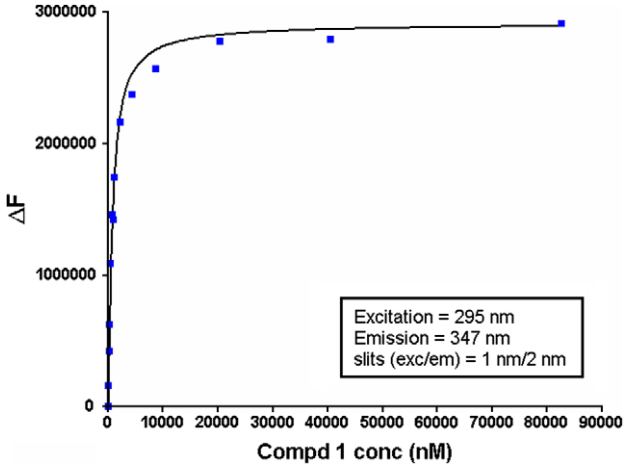

Figure 2. Fluorescence binding experiment: Graph displays fluorescence intensity of 1 μM IGF-1R with compound **1**. Compound **1** binds to IGF-1R with a K_D of 614 nM.

indicated **1** bound to IGF-1R in the submicromolar range (Fig. 2, $K_D = 0.614$ μM).[9] In addition, co-crystal and molecular modeling studies of **1** provided similar orientations of this small molecule lead in the ATP-binding pocket of the IGFR kinase domain. Fig. 3 displays the key interactions to the kinase determined from the co-crystal structure: (a) Glu1080s backbone carbonyl oxygen and **1**'s core NH, (b) Met1082's backbone NH and **1**'s core carbonyl oxygen and (c) Met1082's backbone carbonyl oxygen and **1**'s anilino NH.[10]

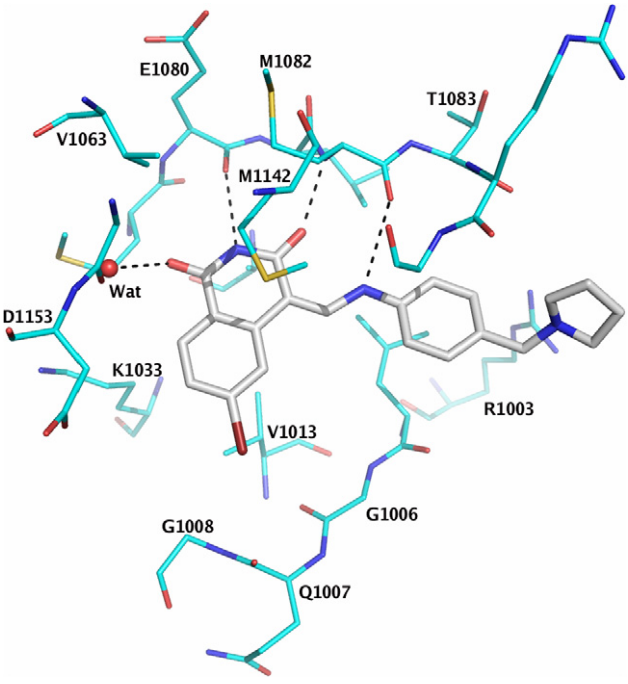

Figure 3. Co-crystal structure of compound **1** in IGF-1R. The key interactions are: (a) Glu1080's O and **1**'s NH, (b) Met1082's NH and **1**'s O, and (c) Met1082's O and **1**'s NH.

Data-mining and clustering techniques using the Wyeth compound database were crucial in determining key functional areas of the molecule; replacement of the bromine of **2** (analog of **1**) with the 6-anilino linkage of **5** (Table 1) provided enhanced activity for IGF-1R versus CDK4, the program from which our equity originated[8] (i.e., **2**: ~3-fold selective for CDK4 and **5**: ~7-fold selective for IGF-1R; also **1**: ~10-fold selective for CDK4). Using structure-based design techniques, the initial libraries (analogs **3 and 4**, and **6–30**) established the SAR around this anilino group with compounds **5**, **8**, and **15** being the most potent initially in this series of IGFR inhibitors. No clear electronic preference was apparent and from molecular modeling analysis, it was rationalized that potency was directly proportional to anilino-NH binding to the protein backbone; the more potent analogs provided optimum alignment of anilino-NH with ASP1153 (i.e., ~3.74 Å distance for **5**, **8**, and **15**).

From analogs **3** and **4** in Table 1, it was apparent that a basic amine in the tailpiece region of the molecule was crucial for inhibitory activity. Our final library (analogs **31**–**41**) was designed to further establish this importance, highlighting that many different tertiary amines were tolerated. Table 1 also summarizes selectivity versus IR for selected analogs; however, to this point, no apparent window of selectivity has been achieved. Interestingly, even our most potent IGFR analog (**39**) showed only a slight preference for IGFR versus IR. With such small differences in the kinase backbone between IGF-1R and IR [Thr1083 (IR Ala) and Arg1084 (IR His)], we are in the process of trying to better understand the minor selectivity preference of **39** with the hopes of obtaining future analogs with a more desirable selectivity window. In addition, aqueous solubility (~1 mg/mL at pH 7.4 for **39**) still needs to be addressed for this series to meet our desired lead profile.

Compounds were prepared by a five-step sequence outlined in Scheme 1.[11] To generate the isoquinolinedione core (**42**), diethyl carbonate was reacted with 4-bromo-2-methyl-benzoic acid in the presence of LDA followed by heating with urea in 1,2-dichlorobenzene at elevated temperature. Further heating this intermediate with triethyl orthoformate in DMF:Ac_2O (4:1) provided compound **43**. Phenylamino-tails **A** or **B** (see Scheme 2) were added to this intermediate followed by addition of the appropriate substituted aniline to afford the final products (see Table 1).

In summary, following a Lance enzyme HTS of the corporate database, full hit characterization of the po-

Table 1. IGFR inhibitory activity and selectivity data versus IR

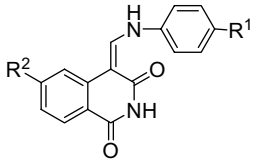

Compound	R^1	R^2	IGFR IC_{50}[a] (μM)	Sel. ratio (IR/IGFR)[b]
1	CH_2-pyrrolidine	Br	2.42	0.57
2	CH_2-piperidine	Br	2.89	nt[c]
3	H	*m*-Cl-aniline	>10	nt[c]
4	H	*m*-MeO-aniline	>10	nt[c]
5	CH_2-piperidine	Aniline	0.455	0.87
6	CH_2-piperidine	*o*-Me-aniline	4.14	nt[c]
7	CH_2-piperidine	*m*-Me–aniline	>10	nt[c]
8	CH_2-piperidine	*p*-Me-aniline	0.498	1.14
9	CH_2-piperidine	*o*-OMe-aniline	0.610	nt[c]
10	CH_2-piperidine	*m*-OMe-aniline	1.08	nt[c]
11	CH_2-piperidine	*p*-OMe-aniline	0.971	nt[c]
12	CH_2-piperidine	*o*-CN-aniline	4.20	nt[c]
13	CH_2-piperidine	*m*-CN-aniline	1.13	nt[c]
14	CH_2-piperidine	*p*-CN-aniline	1.33	nt[c]
15	CH_2-piperidine	*m*-Ac-aniline	0.438	0.72
16	CH_2-piperidine	*p*-Ac-aniline	5.89	nt[c]
17	CH_2-piperidine	*o*-Cl-aniline	1.66	nt[c]
18	CH_2-piperidine	*m*-Cl-aniline	2.39	nt[c]
19	CH_2-piperidine	*p*-Cl-aniline	>10	nt[c]
20	CH_2-piperidine	*m*-F-aniline	2.63	nt[c]
21	CH_2-piperidine	*m*-CF_3-aniline	>10	nt[c]
22	CH_2-piperidine	*m*-NH_2-aniline	>10	nt[c]
23	CH_2-piperidine	*p*-$N(CH_3)_2$-aniline	>10	nt[c]
24	CH_2-piperidine	*p*-$CONH_2$-aniline	0.957	nt[c]
25	CH_2-piperidine	*p*-CO_2Et-aniline	>10	nt[c]
26	CH_2-piperidine	3-OMe-5-CF_3-aniline	>10	nt[c]
27	CH_2-piperidine	5-NH-(1-quinoline)	5.20	nt[c]
28	CH_2-piperidine	5-NH-indole	>10	nt[c]
29	CH_2-piperidine	3,4 ring -$(CH_2)_3$-aniline	7.93	nt[c]
30	CH_2-piperidine	3,4 ring -OCH_2O-aniline	0.894	nt[c]
31	CH_2-NMe_2	Br	7.17	0.58
32	CH_2-piperidine	3-furyl	0.715	0.75
33	*N*-Me-piperazine	Ph-SO_2NH	0.829	0.83
34	3,5-di-Me-piperazine	3-furyl	0.629	1.0
35	CH_2–NMe_2	Aniline	0.920	0.62
36	CH_2–NMe_2	*m*-MeO-aniline	1.39	0.48
37	CH_2–NMe_2	*p*-MeO-aniline	0.566	0.69
38	CH_2–NMe_2	*m*-Ac-aniline	0.887	0.87
39	*N*-Me-piperazine	*m*-Ac-aniline	0.319	1.6
40	3,5-Di-Me-piperazine	*m*-Ac-aniline	0.540	0.85
41	CH_2–NEt_2	*p*-Me-aniline	1.16	0.64

[a] Concentration inducing 50% inhibition of IGFR ($N = 2$–3).[8]
[b] Selectivity ratio (IC_{50} IR inhibition/IC_{50} IGFR inhibition).
[c] nt, not tested in IR inhibition assay.

tential equity generated a novel kinase template as an IGFR inhibitor. Chemical triage and parallel synthesis incorporating focused libraries helped to establish the SAR around this isoquinolinedione core. The key anilino functionality provided compounds (i.e., **5**) with submicromolar activity; however, future analogs around compounds such as **39** will need to be designed with the aim of hopefully improving its selectivity versus IR.

Acknowledgments

We are grateful to the Discovery Analytical Chemistry department of Wyeth Research for elemental analyses, ^{1}H NMR, and mass spectroscopy and Dr. John A. Butera, Dr. John Ellingboe, Mr. Eric Gundersen, Ms. Lori Miller, Ms. Joan Sabalski, and Mr. Gengcheng Yang for scientific discussions.

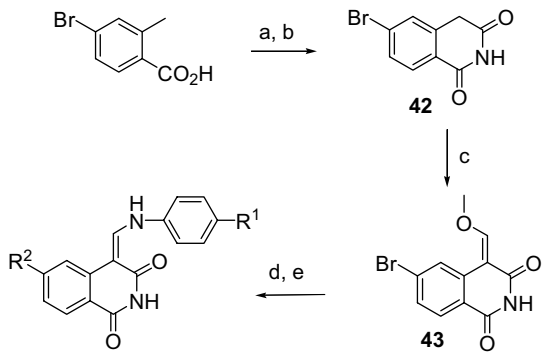

Scheme 1. Reagents and conditions: (a) i—LDA, diethyl carbonate, THF; ii—H_2O; iii—H^+; (b) 1,2-dichlorobenzene, urea, 150 °C; (c) triethylorthoformate, DMF:Ac_2O(4:1), 125 °C; (d) phenylamino-tail **A** or **B** (see Scheme 2), DMF, 110 °C; (e) substituted aniline, KO*t*-Bu, NMP, [1,1′-bis(diphenylphosphino)- ferrocene]dichloro-palladium (II) complex with CH_2Cl_2 (1:1), IPr·HCl·Pd.

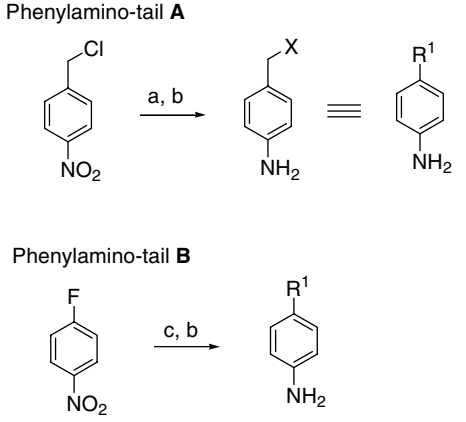

Scheme 2. Reagents and conditions: (a) substituted amine XH, THF, Et_3N; (b) 10% Pd/C, H_2, MeOH; (c) substituted amine R^1H, DMF, K_2CO_3.

References and notes

1. (a) Slamon, D. J.; Leyland-Jones, B.; Shak, S.; Fuchs, H.; Paton, V.; Bajamonde, A.; Fleming, T.; Eiermann, W.; Wolter, J.; Pegram, M.; Baselga, J.; Norton, L. *N. Engl. J. Med.* **2001**, *344*(11), 783; (b) Romond, E. H.; Perez, E. A.; Bryant, J.; Suman, V. J.; Geyer, C. E., Jr.; Davidson, N. E.; Tan-Chiu, E.; Martino, S.; Paik, S.; Kaufman, P. A.; Swain, S. M.; Pisansky, T. M.; Fehrenbacher, L.; Kutteh, L. A.; Vogel, V. G.; Visscher, D. W.; Yothers, G.; Jenkins, R. B.; Brown, A. M.; Dakhil, S. R.; Mamounas, E. P.; Lingle, W. L.; Klein, P. M.; Ingle, J. N.; Wolmark, N. *N. Engl. J. Med.* **2005**, *353*(16), 1673; (c) Johnston, J. B.; Navaratnam, S.; Pitz, M. W.; Maniate, J. M.; Wiechec, E.; Baust, H.; Gingerich, J.; Skliris, G. P.; Murphy, L. C.; Los, M. *Curr. Med. Chem.* **2006**, *13*(29), 3483; (d) Haber, D. A.; Bell, D. W.; Sordella, R.; Kwak, E. L.; Godin-Heymann, N.; Sharma, S. V.; Lynch, T. J.; Settleman, J. *Cold Spring Harb. Symp. Quant. Biol.* **2005**, *70*, 419.
2. Randhawa, R.; Cohen, P. *Mol. Genet. Metab.* **2005**, *86*(1–2), 84.
3. Blakesley, V. A.; Scrimgeour, A.; Esposito, D.; Le Roith, D. *Cytokine Growth Factor Rev.* **1996**, *7*(2), 153.
4. (a) Chng, W. J.; Gualberto, A.; Fonseca, R. *Leukemia* **2006**, *20*(1), 174; (b) Strömberg, T.; Ekman, S.; Girnita, L.; Dimberg, L. Y.; Larsson, O.; Axelson, M.; Lennartsson, J.; Hellman, U.; Carlson, K.; Österborg, A.; Vanderkerken, K.; Nilsson, K.; Jernberg-Wiklund, H. *Blood* **2006**, *107*(2), 669; (c) Breuhahn, K.; Longerich, T.; Schirmacher, P. *Oncogene* **2006**, *25*(27), 3787; (d) Fang, J.; Zhou, Q.; Shi, X.; Jiang, B. *Carcinogenesis* **2007**, *28*(3), 713.
5. (a) Fürstenberger, G.; Senn, H.-J. *Lancet—Oncology* **2002**, *3*, 298; (b) Blum, G.; Gazit, A.; Levitzki, A. *J. Biol. Chem.* **2003**, *278*, 40442; (c) Pollak, M. N.; Schernhammer, E. S.; Hankinson, S. E. *Nat. Rev. Cancer* **2004**, *4*, 505; (d) Garber, K. *J. Nat. Cancer Inst.* **2005**, *97*, 790; (e) Yeh, A. H.; Bohula, E. A.; Macaulay, V. M. *Oncogene* **2006**, *25*(50), 6574; (f) Sachdev, D.; Hartell, J. S.; Lee, A. V.; Zhang, X.; Yee, D. *J. Biol. Chem.* **2004**, *279*(6), 5017; (g) Sachdev, D.; Li, S.-L.; Hartell, J. S.; Fujita-Yamaguchi, Y.; Miller, J. S.; Yee, D. *Cancer Res.* **2003**, *63*(3), 627; (h) Höpfner, M.; Sutter, A. P.; Huether, A.; Baradari, V.; Scherübl, H. *World J. Gastroenterol.* **2006**, *12*(35), 5635; (i) Höpfner, M.; Huether, A.; Sutter, A. P.; Baradari, V.; Schuppan, D.; Scherübl, H. *Biochem. Pharmacol.* **2006**, *71*(10), 1435.
6. De Meyts, P.; Whittaker, J. *Nat. Rev. Drug Discov.* **2002**, *1*, 769.
7. IGF-1R and IR kinase assays: The catalytic domains of IGF-1R or IR were cloned described in Pautsch et al.[12] into pAcG2T [BD Biosciences (San Jose, CA)]. GST-IGF-1R and GST-IR fusion proteins were isolated by glutathione bead capture, eluted, incubated in 20 mM Tris–HCl, pH 7.5, 0.2 M NaCl, 0.01 M $MgCl_2$ and 7.5 mM ATP for 12 min. followed by thrombin cleavage, purification on a glutathione column and MonoQ fractionation. IGF-1R or IR catalytic domains phosphorylated on all three tyrosines in the activation loop as determined by mass spectrometry were then purified on a Superdex 200 column. This ''tris'' phosphorylated protein was used in enzyme assays at 0.6 ng per reaction in 50 mM Hepes, pH 7.5, 0.01 M $MgCl_2$with 150 μg/mL of bovine serum albumin (Sigma #A-8918) and peptide at a final concentration of 1 μg/mL (Biotin–NH_2–TRDIYETDYYRK–OH) for 90 min at room temperature. The final ATP concentration was 100 μM.
8. Originally came from our in-house CDK4 program equity –Tsou; H.-R.; Otteng, M.; Tran, T.; Floyd, M. B. Jr.; Reich, M.; Birnberg, G.; Kutterer, K.; Ayral-Kaloustian, S.; Ravi, M.; Nilakantan, R.; Grillo, M.; McGinnis, J. P.; Rabindran, S. K. *J. Med. Chem.*, in press.
9. Jamieson, E. R.; Jacobson, M. P.; Barnes, C. M.; Chow, C. S.; Lippard, S. J. *J. Biol. Chem.* **1999**, *274*, 12346.
10. RCSB Protein Data Bank (PDB) deposition number 2ZM3.
11. *Experimental:* The synthesis of compound **39** described here serves as a representative example of the synthetic methodology used in this paper.
    Step 1: 4-Bromo-2-carboxylmethyl-benzoic acid. To a stirring solution of diisopropylamine (47.4 g, 465 mmol) in dry THF at −78 °C was added dropwise *n*-butyl lithium (37.3 g, 581 mmol). Mixture was stirred at −78 °C for 0.5 h and then allowed to warm to 25 °C for 5 min causing a yellow suspension to form. Suspension was cooled to −78 °C. 4-Bromo-2-methyl-benzoic acid (25.0 g, 116 mmol) and diethylcarbonate (10.5 g, 116 mmol) were dissolved together in 100 ml of dry THF. This solution was added dropwise to the reaction mixture over 30 min causing a deep reddish-brown color. The resulting mixture was stirred at −78 °C for 1 h and then allowed to warm to room temperature causing a precipitate to form. Mixture

was stirred overnight at room temperature and then cooled in an ice bath. 400 mL of water was slowly added to the mixture keeping the internal temperature below 20 °C causing two layers to form. The layers were separated. The organic layer was extracted with 150 ml of H_2O, and all aqueous layers were combined. Aqueous layers were acidified with concd HCl causing an off-white solid to form. This solid was filtered and washed with 200 ml of H_2O to afford the desired product (18.6 g, 71.8 mmol, 62%); ^{1}H NMR (DMSO-d_6) δ 3.51 (s, 2H), 7.32 (d, J = 2.0 Hz, 1H), 7.39 (dd, J = 1.7, 8.5 Hz, 1H), 7.51 (d, J = 8.4 Hz, 1H).

Step 2: 6-Bromo-4H-isoquinoline-1,3 dione (**42**). 4-Bromo-2-carboxylmethyl-benzoic acid (5.00 g, 19.0 mmol) and urea (2.45 g, 40.8 mmol) were suspended in 150 ml of 1,2-dichlorobenzene. This mixture was heated to 150 °C forming a homogeneous mixture. Temperature was maintained for 2 h during which time a yellow precipitant formed. Mixture was cooled to room temperature and filtered. Residue was washed with 100 ml of ethyl acetate, 100 ml of methanol, and 100 ml of water to afford the product as a yellow solid (3.80 g, 15.8 mmol, 83%); ^{1}H NMR (DMSO-d_6) δ 4.01 (s, 2H), 7.65–7.69 (m, 2H), 7.89 (d, J = 8.7 Hz, 1H), 11.36 (s, 1H).

Step 3: 6-Bromo-4-methoxymethylene-4H-isoquinoline-1,3-dione (**43**). 6-Bromo-4*H*-isoquinoline-1,3-dione (120 mg, 0.500 mmol) and trimethyl orthoformate (106 mg, 1.00 mmol) were suspended in 1.25 ml of a 1:4 ratio mixture of acetic anhydride and dimethylformamide. Mixture was heated at 125 °C for 2 hours causing a yellow solid to form. Mixture was cooled to room temperature and filtered. Residue was washed with 20 ml of ethyl ether to afford the product as a yellow solid (109 mg, 0.380 mmol, 77%); ^{1}H NMR (DMSO-d_6) δ 4.25 (s, 3H),7.60 (dd, J = 1.9, 8.4 Hz, 1H), 7.96 (d, J = 8.5 Hz, 1H), 8.07 (s, 1H), 8.36 (d, J = 1.9 Hz, 1H), 11.38 (s, 1H); mass spectrum [(+)ESI], m/z 282/284 $(M+H)^+$.

Step 4: 6-Bromo-4-{4-(4-methyl-piperazin-1-yl)-phenylamino]methylene}-*4H- isoquinoline-1,3-dione*. 6-Bromo-4-methoxymethylene-4*H*-isoquinoline-1,3-dione (1.46 g, 5.18 mmol) and 4-(4-methyl-piperazin-1-yl)-phenylamine (990 mg, 5.18 mmol) were suspended in 20 ml of dimethylformamide. Mixture was heated at 110 °C for 2 h forming a homogeneous mixture. Mixture was cooled to room temperature and reduced on a rotovap to yield an oil. The residue was diluted with H_2O and stirred for 10 min. The resulting solid was filtered off and washed with H_2O and excess Et_2O to provide the product as a yellowish-brown solid (1.98 g, 86%); ^{1}H NMR (DMSO-d_6) δ 2.19 (s, 3H), 2.42–2.47 (m, 4H), 3.10–3.16 (m, 4H), 6.95 (d, J = 9.0 Hz, 2H), 7.33 (dd, J = 1.7, 8.5 Hz, 1H), 7.43 (d, J = 9.0 Hz, 2H), 7.86 (d, J = 8.5 Hz, 1H), 8.38 (d, J = 1.74 Hz, 1H), 8.84 (d, J = 12.9 Hz, 1H), 11.28 (s, 1H), 12.54 (d, J = 12.9 Hz, 1H); mass spectrum [(+)ESI], m/z 441/443 $(M+H)^+$.

Step 5: 4-{4-(4-methyl-piperazin-1-yl)-phenylamino]-methylene} -6-m-acetylphenylamino-4H-isoquinoline-1,3-dione (**39**). 6-Bromo-4-{4-(4-methyl-piperazin-1-yl)-phenylamino]methylene}-4*H*- isoquinoline-1,3-dione (300 mg, 0.680 mmol), 3-amino-acetophenone (184 mg, 1.36 mmol), allylchloro{1,3-bis(2,6-di-propylphenyl)imidazol-2- yilidine]palladium(II) (IPr·HCl·Pd, 78 mg, 0.136 mmol), [1,1′-bis(diphenylphosphino)-ferrocene]dichloro-palladium (II) complex with CH_2Cl_2 (1:1) (56 mg, 0.0680 mmol), and potassium-*t*-butoxide (229 mg, 2.04 mmol) were all dissolved in 3.0 ml of *N*-Methyl-2-pyrolidinone. Mixture was heated at 150 °C in a microwave for 15 min using normal absorption and fixed hold on. The resulting solution was purified by silica gel chromatography (eluent: 1–20% MeOH:$CHCl_3$) followed by preparatory plate chromatography (eluent: 10% MeOH:$CHCl_3$) to afford the product as a brownish solid (29 mg, ~10%), mp 268–270 °C; ^{1}H NMR (DMSO-d_6) δ 2.19 (s, 3H), 2.36–2.48 (m, 4H), 2.54 (s, 3H), 3.04–3.16 (m, 4H), 6.88–6.99 (m, 3H), 7.29 (d, J = 9.0 Hz, 2H), 7.39–7.48 (m, 2H), 7.49–7.54 (m, 2H), 7.73 (s, 1H), 7.85 (d, J = 8.7 Hz, 1H), 8.46 (d, J = 12.8 Hz, 1H), 8.83 (s, 1H), 10.89 (s, 1H), 12.28 (d, J = 12.9 Hz, 1H); mass spectrum [(+)ESI], m/z 496 $(M+H)^+$; Anal. Calcd for $C_{29}H_{29}N_5O_3 \cdot 0.5CH_2Cl_2$: C, 65.85; H, 5.62; N, 13.02 Found: C, 66.00; H, 4.99; N, 12.72.

12. Pautsch, A.; Zoephel, A.; Ahorn, H.; Spevak, W.; Hauptmann, R.; Nar, H. *Structure* **2001**, *9*(10), 955.